Suppression of tumor growth by GMI, an edible fungal immunomodulatory protein, is associated with targeting GSK3β-mediated proteasomal degradation of PD-L1

WEI-JYUN HUA[1,2], LI-CHEN HUANG[1], ZHI-HU LIN[1,2], YI-RU CIOU[1], KAI-FAN LIN[1], LI-LAN LIAO[1,3], WEI-HUNG HSU[1,4-6] and TUNG-YI LIN[1,2,4,7]

[1]Institute of Traditional Medicine, National Yang Ming Chiao Tung University, Taipei 11221, Taiwan, R.O.C.; [2]Traditional Chinese Medicine Glycomics Research Center, National Yang Ming Chiao Tung University, Taipei 11221, Taiwan, R.O.C.; [3]Branch of Linsen Chinese & Kunming, Taipei City Hospital, Taipei 108203, Taiwan, R.O.C.; [4]School of Chinese Medicine, National Yang Ming Chiao Tung University, Taipei 11221, Taiwan, R.O.C.; [5]Department of Traditional Chinese Medicine, Lo-Sheng Sanatorium and Hospital, Ministry of Health and Welfare, Taoyuan 33351, Taiwan, R.O.C.; [6]School of Oral Hygiene, College of Oral Medicine, Taipei Medical University, Taipei 11031, Taiwan, R.O.C.; [7]Biomedical Industry Ph.D. Program, National Yang Ming Chiao Tung University, Taipei 11221, Taiwan, R.O.C.

Received May 12, 2025; Accepted September 26, 2025

DOI: 10.3892/ijmm.2025.5658

Abstract. Cancer cells evade T cell responses by exploiting programmed death-ligand 1 (PD-L1) in the tumor microenvironment, and oncogenic epidermal growth factor receptor (EGFR) signaling stabilizes PD-L1 expression. *Ganoderma microsporum* immunomodulatory protein (GMI), a consumable mushroom-derived dietary supplement, functions as an EGFR degrader targeting EGFR-positive cancer cells. However, the role of GMI in regulating PD-L1 and modulating antitumor immunity has not been fully elucidated. In the present study, functional enrichment analysis was first employed to investigate GMI-regulated differentially expressed proteins. The findings indicated that GMI may modulate the PD-L1 signaling pathway. GMI downregulated PD-L1 expression by regulating both mRNA and protein stability, thereby suppressing PD-L1-positive lung cancer cells *in vitro* and *in vivo*. Functional studies further demonstrated that GMI promotes glycogen synthase kinase 3 beta (GSK3β)-mediated proteasomal degradation of PD-L1. Knockdown of GSK3β in lung cancer cells abolished the GMI-induced reduction in PD-L1 expression. Additionally, GMI inhibited tumor growth and reduced PD-L1 levels in allograft mouse models. Importantly, GMI-mediated PD-L1 downregulation correlated with enhanced T cell-mediated inhibition of lung cancer cells. These findings shed light on the potential of edible GMI to boost antitumor immunity.

Correspondence to: Professor Tung-Yi Lin, Institute of Traditional Medicine, National Yang Ming Chiao Tung University, 155 Li-Nung Street, Section 2, Shipai, Beitou, Taipei 11221, Taiwan, R.O.C.
E-mail: biotungyi@gmail.com; tylin99@nycu.edu.tw

Abbreviations: GMI, *Ganoderma microsporum* immunomodulatory protein; PD-L1, programmed death-ligand 1; EGFR, epidermal growth factor receptor; FIPs, fungal immunomodulatory proteins; PD-1, programmed cell death protein-1; GSK3β, glycogen synthase kinase 3 beta; LiCl, lithium chloride; KEGG, Kyoto Encyclopedia of Genes and Genomes; NSCLC, non-small cell lung cancer; DEPs, differentially expressed proteins; TILs, tumor-infiltrating lymphocytes

Key words: GMI, lung cancer, PD-L1 degradation, proteasomal pathway, antitumor immunity

Introduction

Cancer cells cleverly evade T cell-mediated immune responses by manipulating immune cells and leveraging immune checkpoints to communicate with the host's defense mechanisms within the tumor microenvironment (TME) (1). This process disrupts immune surveillance, allowing tumors to escape detection and avoid destruction. A critical component in this mechanism is programmed death-ligand 1 (PD-L1; also known as B7-H1 or CD274), a membrane glycoprotein frequently overexpressed across various cancer types. PD-L1 acts as a critical immune checkpoint molecule through its interaction with programmed cell death protein-1 (PD-1; also called CD279), which is expressed on the surface of activated T lymphocytes (2). This interaction inhibits the activation of cytotoxic T cells, impairing the immune system's ability to identify and eliminate cancer cells. By hijacking this pathway, cancer cells can effectively evade immune eradication, thereby promoting their survival and enabling further progression (3).

Immunotherapies targeting PD-1 or PD-L1 with antibodies have shown significant and durable clinical responses in treating various cancers, including non-small cell lung cancer (NSCLC), melanoma and renal cell carcinoma (4,5).

These therapies function by inhibiting the binding of PD-1 on immune cells to PD-L1 on tumor cells, thereby enhancing the immune system's ability to recognize and eradicate cancer cells. The success of immune checkpoint blockade highlights its potential to transform cancer treatment paradigms, providing new options for patients who previously had limited alternatives (6). However, despite their notable efficacy, these therapies do not benefit all patients and face limitations such as poor tumor tissue penetration, adverse immune reactions and lack of oral bioavailability (7). Additionally, targeting PD-L1 for degradation, rather than merely blocking its interaction with PD-1, might offer a more effective strategy by thoroughly disrupting the PD-1/PD-L1 signaling axis, potentially enhancing therapeutic efficacy (8,9).

PD-L1 expression is regulated through multiple mechanisms, including the activation of oncogenic transcription factors such as c-Myc and NF-κB, which promote PD-L1 upregulation at the gene transcription level. Additionally, post-translational modifications, such as glycosylation and ubiquitination, are essential for stabilizing PD-L1 and regulating its functional protein levels (10). For example, activating β-catenin during epithelial-mesenchymal transition (EMT) induces the transcription and synthesis of the STT3 gene (a catalytic subunit of the oligosaccharyltransferase (OST) complex). This, in turn, promotes PD-L1 glycosylation, thereby inhibiting its degradation in cancer stem cells (11). Furthermore, cyclin D-CDK4 and glycogen synthase kinase 3 beta (GSK3β) facilitate PD-L1 ubiquitination, marking it for proteasomal degradation (12,13). Notably, the oncogenic epidermal growth factor receptor (EGFR) plays a key role in regulating PD-L1 expression. Inhibition of EGFR signaling destabilizes PD-L1 through GSK3β activation, ultimately enhancing antitumor immunity (14). These findings suggested that agents targeting EGFR may represent a promising approach to enhance immune responses by promoting PD-L1 degradation.

GMI, a fungal immunomodulatory protein (FIP) from *Ganoderma microsporum*, is a dietary supplement with both nutritional and therapeutic benefits (15). Beyond its origin as an edible mushroom, GMI has drawn significant attention for its diverse biological properties, especially its potent anticancer activity. GMI downregulates heat shock protein expression, which is associated with apoptosis in lung cancer cells (16). In addition, it has shown synergistic anticancer effects when combined with therapeutic agents such as temozolomide and sotorasib in glioblastoma multiforme (GBM) and $KRAS^{G12C}$ mutant lung cancers, respectively (17,18). GMI has been identified as an EGFR degrader capable of disrupting EGFR-driven oncogenic signaling and suppressing tumor growth in EGFR-positive cancers (19). However, whether GMI regulates PD-L1 expression and enhances antitumor immune responses remains unclear.

In the present study, the effects of GMI on PD-L1 expression were investigated and it was found that it promotes GSK3β-mediated proteasomal degradation of PD-L1, leading to reduced membrane PD-L1 levels. Furthermore, GMI enhances T cell-mediated suppression of tumor cells. These findings collectively suggested that GMI may serve as a functional food with potential therapeutic benefits for enhancing antitumor immunity through modulating PD-L1 expression.

Materials and methods

Reagents. GMI was produced by MycoMagic Biotechnology. The purification procedures and the detailed structural characterization (Protein Data Bank ID: 3KCW) have been previously documented (20). Bafilomycin A1 (Baf A1) and cycloheximide (CHX) were purchased from MilliporeSigma. MG132 and lithium chloride (LiCl) were obtained from ITW Reagents (PanReac AppliChem) and Enzo Life Sciences, respectively. LY294002 and Osimertinib were purchased from MedChemExpress and TargetMol, respectively. Anti-mouse PD-1 antibody (CD279; clone RMP1-14) was purchased from Bio X Cell.

Experimental cell lines and culture conditions. Lewis lung carcinoma (LLC1), GBM8401 and Jurkat T cells were obtained from the Bioresource Collection and Research Center. A549 cell line was purchased from the American Type Culture Collection. H1975 and T98G cells were obtained from Elabscience Biotechnology, Inc. and the Japanese Cancer Research Resources Bank, respectively. PC9 and CL1-5 cells were generously provided by Dr Tsai of the National Yang Ming University and Dr P.C. Yang of the National Taiwan University, respectively. U87, a human glioblastoma cell line of unknown origin (21), was kindly provided by Dr T.H. Tu of Taipei Veterans General Hospital. The LLC1-hPD-L1 cell line was a gift from Dr K.L. Lan of the National Yang Ming Chiao Tung University.

LLC1-hPD-L1 cells were cultured in Dulbecco's Modified Eagle's Medium supplemented with 10% fetal bovine serum (VWR Life Science Seradigm), 1% penicillin/streptomycin, 1% sodium pyruvate, 1% L-glutamine (all from GIBCO; Thermo Fisher Scientific, Inc.) and 200 μg/ml hygromycin B (MedChemExpress). Short tandem repeat (STR) analysis was used for authentication in H1975, A549 and GBM8401 cell lines. Detailed culture conditions for the other cell lines have been previously described (18,19). All cell cultures were incubated at 37˚C in a humidified environment containing 5% CO_2.

Kyoto Encyclopedia of Genes and Genomes (KEGG) analysis. The extraction of membrane proteins used for LC-MS/MS analysis has been previously described (22). Briefly, membrane proteins were extracted from GMI-treated cells and subjected to proteomic analysis. Differentially expressed proteins (DEPs) regulated by GMI were identified based on a fold change (GMI/CTL) of <0.75 or >1.33. These DEPs were then analyzed for pathway enrichment using ShinyGO V0.80 (23), and the selected enriched pathway was visualized using KEGG diagrams, with DEPs highlighted in red (24,25).

Western blotting and immunoprecipitation (IP) assay. Western blot analysis was performed as previously described (26). In brief, treated cells were harvested and lysed in a cell lysis buffer containing protease and phosphatase inhibitors (MilliporeSigma). The lysates were cleared by centrifugation at 16,200 x g for 10 min at 4˚C, and protein concentrations in the supernatants were quantified prior to analysis using the Bradford protein assay (Bio-Rad Laboratories, Inc.), with bovine serum albumin (BSA; Thermo Fisher Scientific, Inc.) as the calibration standard. Subsequently, 30 μg of total protein

from each sample was separated by 10% SDS-polyacrylamide gel electrophoresis and transferred onto PVDF membranes (0.45 μm; MilliporeSigma). The membranes were incubated with primary antibodies at 4˚C overnight, followed by incubation with species-specific secondary antibodies at room temperature for 1 h prior to chemiluminescence detection. For IP assay, cells were pretreated with a proteasome inhibitor, followed by GMI treatment for the indicated time. Cell lysates were prepared and centrifuged in IP lysis buffer containing EDTA at 16,200 x g for 10 min at 4˚C. Then, 400 μg of supernatant was incubated overnight at 4˚C with a PD-L1 antibody (1:50) for immunoprecipitation. Ubiquitinated PD-L1 was subsequently detected by western blotting. Antibodies for detecting PD-L1 (rabbit; 1:1,000; cat. no. 13684), phosphorylated (p-)GSK3β (Ser 9; rabbit; 1:1,000; cat. no. 5558), p-AKT (Ser473; rabbit; 1:1,000; cat. no. 4060), p-EGFR (Tyr1068; rabbit; 1:1,000; cat. no. 3777) and ubiquitin (mouse; 1:1,000; cat. no. 3936) were acquired through Cell Signaling Technology, Inc. Antibodies specific to GSK3β (rabbit; 1:1,000; cat. no. GTX111192), caveolin (rabbit; 1:1,000; cat. no. GTX100205), EGFR (rabbit; 1:1,000; cat. no. GTX121919), tubulin (rabbit; 1:10,000; cat. no. GTX112141), goat anti-mouse IgG antibody (HRP; 1:10,000; cat. no. GTX213111-01) and goat anti-rabbit IgG antibody (HRP; 1:10,000; cat. no. GTX213110-01) were obtained via GeneTex International Corporation. AKT (rabbit; 1:1,000; cat. IR171-666) antibody was purchased from iReal Biotechnology. Protein band intensities were quantified by densitometric analysis using ImageJ software (version 1.53a; National Institutes of Health), with values normalized to the respective loading controls.

Extraction of plasma membrane PD-L1. The experimental procedures have been previously documented (19). Briefly, plasma membrane proteins were isolated using the Trident Membrane Protein Extraction Kit (GeneTex International Corporation), following the manufacturer's instructions. The extracted membrane proteins were subsequently evaluated using western blot analysis.

Immunofluorescence assay. H1975 and CL1-5 cells ($2x10^4$) were seeded on coverslips and treated with GMI and/or LiCl for 3 h. Cells were then subjected to fixation at room temperature for 15 min with 4% paraformaldehyde (Bioman Scientific Company, Ltd.) and permeabilized in PBS containing 0.1% Triton X-100 (MilliporeSigma) for another 10 min. Blocking was performed with PBS containing 1% BSA for 30 min. Cells were then incubated overnight at 4˚C with anti-PD-L1 primary antibodies (1:400; Abcam; cat. no. ab205921). After washing with PBS supplemented with 0.05% Tween 20, the cells were incubated at room temperature for 1 h with goat anti-rabbit IgG antibody (DyLight488; 1:1,000; GeneTex International Corporation; cat. no. GTX213110-04). Nuclei were visualized by mounting cells with Fluoroshield containing DAPI (Millipore; cat. no. F6057). Observations and imaging were performed using an ImageXpress Pico digital microscope (Molecular Devices, LLC).

Reverse transcription-quantitative PCR (RT-qPCR). Total RNA was extracted using the Quick-RNA Miniprep Kit (Zymo Research Corp.), following the manufacturer's instructions. Complementary DNA (cDNA) synthesis was performed from 500 ng of RNA using the PrimeScript™ RT reagent Kit (Takara Bio, Inc.) in accordance with the manufacturer's protocol. Amplification of the cDNA was performed with TB Green® Premix Ex Taq II (Takara Bio, Inc.) on a StepOnePlus™ Real-Time PCR System (Applied Biosystems; Thermo Fisher Scientific, Inc.). The thermocycling conditions were set as follows: initial denaturation at 95˚C for 30 sec, followed by 40 cycles of denaturation at 95˚C for 5 sec and annealing/extension at 60˚C for 30 sec. The specific primers for the genes of interest were as follows: PD-L1 forward, 5'-CAATGTGACCAGCACACTGAGAA-3' and reverse, 5'-GGCATAATAAGATGGCTCCCAGAA-3'; and GAPDH forward, 5'-TGGTATCGTGGAAGGACTCA-3' and reverse, 5'-AGTGGGTGTCGCTGTTGAAG-3'. Relative PD-L1 mRNA levels were quantified by the comparative $2^{-\Delta\Delta Cq}$ method (27), using GAPDH as the endogenous control and normalized to the control group.

Short hairpin RNA (shRNA) transfection. Lentiviral shRNA transfection was conducted as previously described (18). Briefly, one CTL-shRNA (shCTL; TRCN0000208001; pLKO.1 empty-vector negative control lacking an shRNA hairpin insert) and two GSK3β-shRNA lentivirus constructs were obtained from the National RNAi Core Facility (Taipei, Taiwan) and generated in 293T cells. These lentiviruses were subsequently employed to transduce H1975 and CL1-5 cells, followed by selection with 5 μg/ml puromycin (MilliporeSigma). The target sequences for GSK3β were 5'-AGCAAATCAGAGAAATGAAC-3' (shGSK3β#1; TRCN0000039565) and 5'-CCCAAACTACACAGAATT TAA-3' (shGSK3β#2; TRCN0000039999).

T cell-mediated tumor cell killing assay. T cell cytotoxicity assay was conducted as previously described (28,29). Primary T cells were isolated from the spleens of LLC1-bearing mice using a magnetic cell separation system with the mouse CD3ε MicroBead Kit (Miltenyi Biotec GmbH; cat. no. 130-094-973), following the manufacturer's protocols. Jurkat and isolated T cells were activated for 48 h by incubation with Dynabeads™ Human T-Activator CD3/CD28 (Invitrogen; Thermo Fisher Scientific, Inc.; cat. no. 11161D) and Dynabeads™ Mouse T-Activator CD3/CD28 (Invitrogen; Thermo Fisher Scientific, Inc.; cat. no. 11452D), respectively. Next, GMI-treated green fluorescent protein (GFP)-expressing tumor cells were co-cultured with the activated T cells for 72 h at the following effector-target ratios: 1:2 for LLC1-GFP cells, 1:1 for H1975-GFP cells, and 1:10 for PC9-GFP cells. After removing the supernatant, the cells were washed, trypsinized, centrifuged at 120 x g for 5 min at room temperature, and resuspended in PBS. GFP fluorescence was measured using a Varioskan LUX multimode microplate reader (Thermo Fisher Scientific, Inc.), with excitation set at 485 nm and emission at 520 nm.

Measurement of interleukin-2 (IL-2) and granzyme B secreted by activated Jurkat T cells using a co-culture assay and enzyme-linked immunosorbent assay (ELISA). Jurkat T cells were activated for 48 h using Dynabeads™ Human T-Activator CD3/CD28 (Invitrogen; Thermo Fisher Scientific,

Inc.; cat. no. 11161D). H1975-GFP and PC9-GFP lung cancer cells were pretreated with GMI for 24 h, detached with trypsin, and then co-cultured with activated T cells at a 1:1 ratio for both H1975-GFP and PC9-GFP cells. Supernatants were collected, and levels of secreted IL-2 and granzyme B were measured using Human IL-2 and Granzyme B ELISA Kit (BioLegend, Inc.; cat. no. 431804; and R&D Systems, Inc.; cat. no. DY2906-05, respectively). The assay was conducted according to the manufacturer's protocols, as previously described (20). In addition, to directly examine the effect of GMI on T cell function, Jurkat T cells were treated with GMI for 24 h. Culture supernatants were collected, and IL-2 secretion was measured by ELISA.

Syngeneic tumor model. Animal studies were approved by the Institutional Animal Care and Use Committee (IACUC) at National Yang Ming Chiao Tung University (IACUC approval no. 1070805) and were conducted in accordance with the established guidelines, following procedures as described previously (17). A total of 42 male C57BL/6 (National Laboratory Animal Center, Taipei, Taiwan) mice were used in the present study. The animals were 6-8 weeks of age and weighed 20-22 g at the start of the experiments. They were housed under controlled conditions (temperature 20-22˚C; relative humidity 50±10%) with a 12/12-h light/dark cycle and had free access to food and water. In addition, group sizes were chosen in line with published LLC1 syngeneic practice and institutional guidance, where similar cohort sizes have been sufficient to detect significant differences (30-33). Briefly, mice were subcutaneously injected with $1x10^5$ LLC1 or LLC1-hPD-L1 cells, and then treated intraperitoneally with GMI (5 mg/kg) or vehicle control (PBS) every 3 days. In the tumor model involving GMI with or without anti-PD-1 antibody treatment, mice were randomly divided into four distinct treatment groups: control (CTL), anti-PD-1 mAb (200 μg/mice), GMI (5 mg/kg), and GMI + anti-PD-1 mAb. Treatments were administered every 2 days. Tumor volume was calculated using the formula: length x $width^2$ x 1/2. At the study endpoint, the mice were humanely euthanized by carbon dioxide (CO_2) inhalation using a gradual fill rate of 30-70% of the chamber volume per min without pre-filling, and tumors were excised and weighed.

Tumor-infiltrating lymphocytes (TILs) were isolated from GMI- and PBS-treated LLC1 tumors. Non-specific binding was blocked using CD16/CD32 antibodies (Thermo Fisher Scientific, Inc.; cat. no. 14-0161-82), followed by staining on ice for 30 min with anti-mouse CD3 (BioLegend, Inc.; cat. no. 100235), CD8 (BioLegend, Inc.; cat. no. 100707) and CD4 (BioLegend, Inc.; cat. no. 100405) antibodies, targeting immune markers. Samples were analyzed using a CytoFLEX Flow Cytometer (Beckman Coulter, Inc.) and the $CD8^+/CD4^+$ T cell ratio was determined. In a separate assay, Jurkat T cells were treated with GMI for 24 h, stained with PE anti-human CD69 antibody (BioLegend, Inc.; cat. no. 310905), and subsequently analyzed for surface CD69 expression using flow cytometry.

Statistical analysis. All data were represented as the mean ± standard deviation (SD) from three independent experiments. Comparisons between two groups were performed using two-tailed unpaired Student's t-tests. For comparisons among more than two groups, one-way analysis of variance (ANOVA) was used, followed by appropriate post hoc tests. Specifically, Dunnett's test was applied when all groups were compared with the control group, while Tukey's test was used for comparisons among all groups. Analyses were performed using GraphPad Prism 10 software (Dotmatics). $P<0.05$ was considered to indicate a statistically significant difference.

Results

GMI reduces relative membrane PD-L1 intensity in three lung cancer cell lines. A previous proteomic analysis of membrane protein extractions by the authors revealed that GMI downregulated members of the integrin family in H1975, CL1-5 and A549 lung cancer cells (Fig. 1A) (22). To further characterize the functions of GMI-regulated DEPs, the KEGG pathway enrichment analysis was performed. Among the enriched pathways, the 'PD-L1 expression and PD-1 checkpoint pathway in cancer' was identified (Fig. 1B and Table SI). Within this pathway, PD-L1 and EGFR were downregulated by GMI, while IFNGR1 was upregulated (Figs. 1C and S1, and Table SII). Given that GMI is a known EGFR degrader and that EGFR is closely associated with the regulation of PD-L1 protein levels, the mechanism underlying GMI-induced reduction of membrane PD-L1 intensity was investigated in these three lung cancer cell lines (Fig. 1D).

GMI decreases PD-L1 protein levels in H1975, CL1-5 and A549 cells. A previous study by the authors showed that 0.6 μM GMI markedly modulated EGFR (19); therefore, this dose was selected for subsequent assays. Membrane protein fractionation assays were performed to evaluate the effects of GMI on plasma membrane PD-L1 levels. Consistent with our proteomic findings, a significant decrease in membrane PD-L1 following GMI treatment was observed (Fig. 2A). Immunofluorescence analysis further confirmed that membrane PD-L1 accumulation was significantly reduced in GMI-treated H1975 and CL1-5 cells (Fig. 2B). Furthermore, PD-L1 protein expression was significantly reduced in all examined cell lines after both short-term and long-term exposure to GMI (Fig. 2C and D). Basal PD-L1 levels were assessed across a panel of lung cancer cell lines, revealing relatively lower PD-L1 expression in A549 cells and higher expression in H1975 cells (Fig. S2A), echoing previous studies (34,35). Given that CL1-5 cells exhibited intermediate PD-L1 levels, H1975 and CL1-5 cell lines were selected for further investigation. In GBM cell lines, PD-L1 was highly expressed in GBM8401 cells, minimally expressed in T98G cells, and intermediate in U87 cells (Fig. S2A). Notably, GMI reduced PD-L1 levels in both GBM8401 and U87 cells in a dose-dependent manner (Fig. S2B and C). Collectively, these findings suggested that GMI may play a role in modulating PD-L1 expression by effectively reducing membrane PD-L1 levels.

GMI suppresses PD-L1 mRNA levels and promotes proteasomal PD-L1 degradation. It was next examined whether GMI influences *PD-L1* transcription. RT-qPCR assay revealed an initial increase in *PD-L1* mRNA levels at 1 h, followed by a significant decrease at 24 h post-treatment (Fig. 3A). To

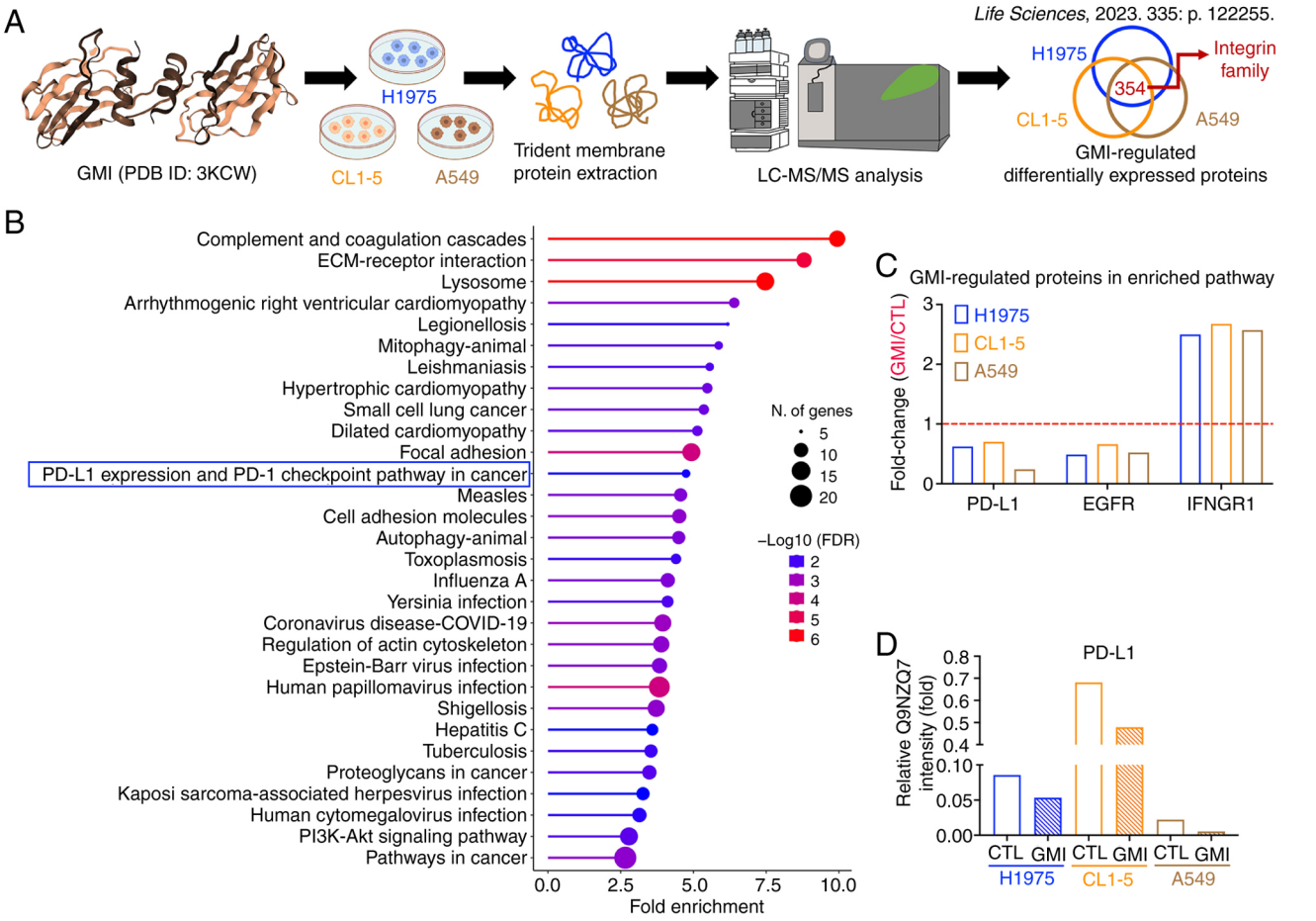

Figure 1. GMI regulates PD-L1 expression in H1975, CL1-5 and A549 lung cancer cells. (A) Schematic workflow of membrane protein extraction from GMI-treated cancer cells, followed by liquid chromatography-mass spectrometry proteomic analysis to identify GMI-regulated DEPs. (B) Kyoto Encyclopedia of Genes and Genomes pathway enrichment analysis of GMI-regulated DEPs, highlighting the top 30 significant pathways ranked by fold enrichment. 'The PD-L1 expression and PD-1 checkpoint pathway in cancer' is highlighted within the blue box. (C) Densitometric analysis showing the fold changes (GMI/CTL) of proteins within the enriched pathway, with two downregulated proteins (fold change <0.75) and one upregulated protein (fold change >1.33). (D) Bar graph depicting relative PD-L1 intensity in GMI-treated lung cancer cells compared with untreated controls. GMI, *Ganoderma microsporum* immunomodulatory protein; PD-L1, programmed death-ligand 1; DEPs, differentially expressed proteins; PD-1, programmed cell death protein-1.

assess the impact of GMI on PD-L1 protein stability, CHX, the protein synthesis inhibitor, was used. The findings of the present study revealed that PD-L1 protein degradation was accelerated in cells exposed to GMI (Fig. 3B), indicating that GMI promotes the post-translational regulation of PD-L1, leading to enhanced protein degradation.

PD-L1 can be degraded through either the proteasomal or lysosomal pathway, both leading to reduced PD-L1 presence on the cell membrane (36). To identify the specific signaling pathway implicated in GMI-mediated PD-L1 reduction, cells were exposed to GMI combined with specific inhibitors: MG132 for proteasomes and Baf A1 for lysosomes. The findings revealed that GMI-triggered acceleration of PD-L1 breakdown was strongly mitigated in the presence of MG132 (Fig. 3C), implicating the proteasomal pathway in this process. By contrast, Baf A1 did not inhibit the degradation (Fig. 3D), indicating that the lysosomal pathway is not significantly involved. Furthermore, under endogenous (non-overexpression) conditions, an in-cell ubiquitination assay showed a slight increase in PD-L1 ubiquitination following GMI treatment, although the effect was not pronounced (Fig. S3A and B). These findings suggested that GMI reduces PD-L1 protein levels not only by suppressing its transcription but also by enhancing the proteasome-dependent system and subsequent degradation.

GMI destabilizes PD-L1 by promoting GSK3β-mediated proteasomal degradation. Activated EGFR induces AKT-mediated phosphorylation of GSK3β at serine 9 (Ser9), rendering it inactive and thereby stabilizing PD-L1 by preventing its proteasomal degradation (37). It was hypothesized that GSK3β signaling contributes to GMI-mediated PD-L1 degradation. The present results demonstrated that GMI, as an EGFR degrader, effectively suppressed EGFR expression and downstream AKT activation (Fig. 4A and B; Fig. S4A and B). Moreover, treatment with GMI (0.6 μM) significantly reduced GSK3β Ser9 phosphorylation after both short-and long-term treatments, indicating GSK3β activation concomitant with PD-L1 suppression (Fig. 4A and B). Similar reductions in PD-L1 expression were observed upon treatment with osimertinib, an EGFR inhibitor, and LY294002, a PI3K/AKT inhibitor (Fig. S4C). Conversely, co-treatment with LiCl, a GSK3β inhibitor, significantly rescued PD-L1 levels reduced by GMI (Fig. 4C), as confirmed by immunofluorescence analysis (Fig. S5). To further validate GSK3β's

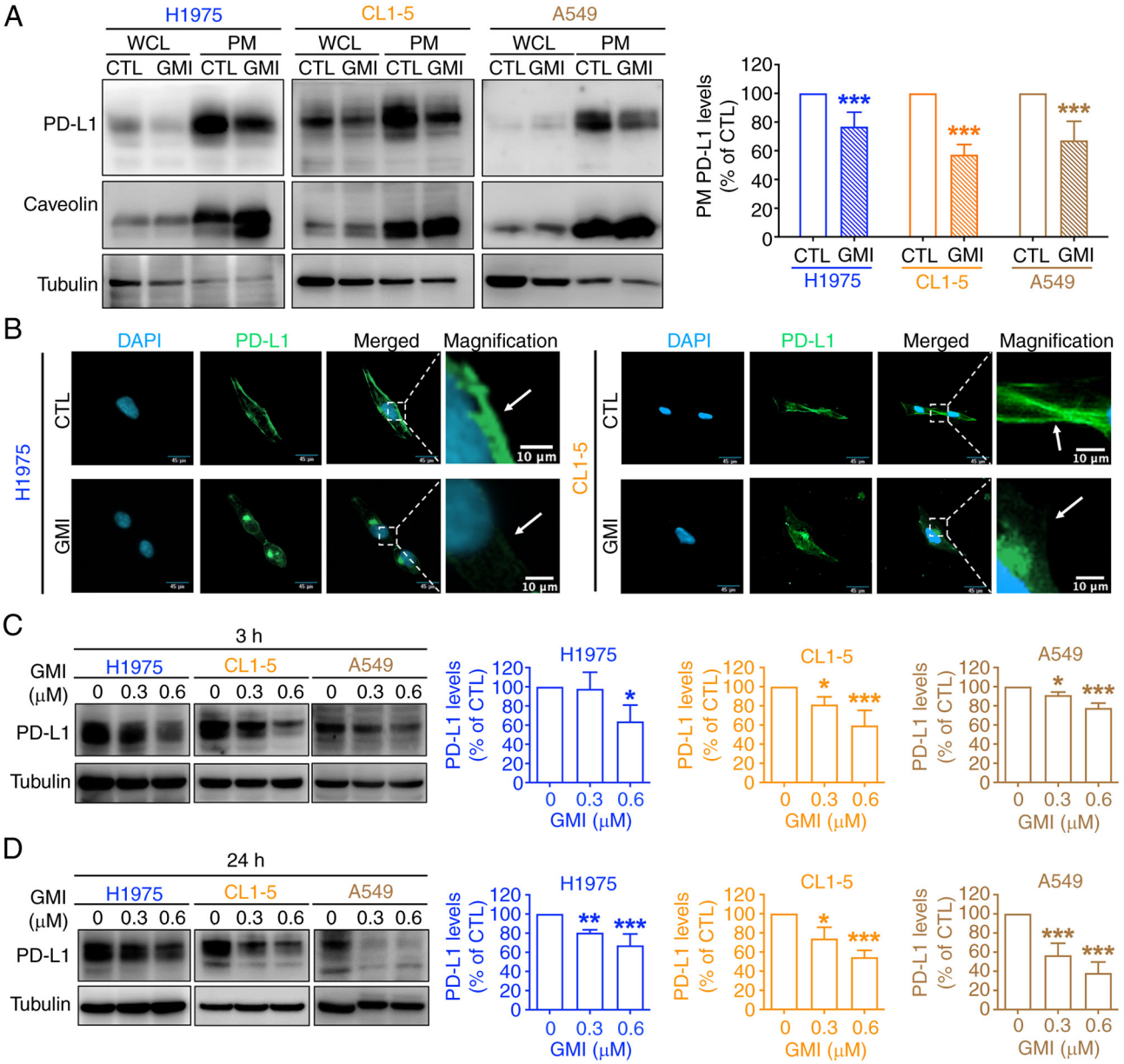

Figure 2. GMI reduces membrane PD-L1 protein levels in lung cancer cells. (A) Left: Immunoblot analysis of PD-L1 in WCL and PM fractions isolated from H1975, CL1-5 and A549 cells after 24 h treatment with 0.6 μM GMI. Caveolin and tubulin were used as markers for PM and WCL fractions, respectively. Right: quantification of PD-L1 levels in PM fractions normalized to caveolin. (B) Immunofluorescence staining of PD-L1 (green) and nuclei (DAPI, blue) in H1975 and CL1-5 cells treated with 0.6 μM GMI for 3 h. Scale bars, 45 μm (main images) and 10 μm (magnified insets). (C and D) Western blot analysis of PD-L1 protein levels in H1975, CL1-5 and A549 cells treated with indicated concentrations of GMI for 3 h (C) and 24 h (D). Tubulin served as the loading control. Data are presented as the mean ± standard deviation from three independent experiments. *P<0.05, **P<0.01 and ***P<0.001. GMI, *Ganoderma microsporum* immunomodulatory protein; PD-L1, programmed death-ligand 1; WCL, whole-cell lysates; PM, plasma membrane.

role, shRNA-mediated knockdown of GSK3β in both H1975 and CL1-5 cells attenuated GMI-induced PD-L1 degradation (Fig. 4D), resulting in elevated PD-L1 compared with GMI-treated parental cells (Fig. 4E and F). Collectively, these findings demonstrated that GSK3β activation is crucial for GMI-induced proteasomal degradation of PD-L1.

GMI suppresses tumor growth and reduces PD-L1 expression in vivo. A previous study by the authors showed that GMI effectively suppressed tumor growth in a LLC1-bearing mouse model (19). In the present study, it was further explored whether GMI can downregulate PD-L1 expression in LLC1 cells both *in vitro* and *in vivo*. First, it was observed that GMI treatment reduced PD-L1 levels in LLC1 cells *in vitro* (Fig. 5A). Subsequently, LLC1-bearing immune-competent C57BL/6 mice were administered GMI or PBS (CTL) via intraperitoneal injection every 3 days (Fig. S6A). The results demonstrated that GMI significantly suppressed tumor growth (Fig. S6B), echoing our previous findings, without affecting overall body weight, thus revealing favorable tolerability of GMI (Fig. S6C). Western blot analysis of harvested tumors revealed that GMI treatment significantly decreased PD-L1 expression compared with the CTL group, indicating that GMI induces PD-L1 degradation in tumor-bearing mice (Fig. 5B).

To further investigate whether GMI-induced degradation of human PD-L1 (hPD-L1) *in vivo*, LLC1-hPD-L1 cells were

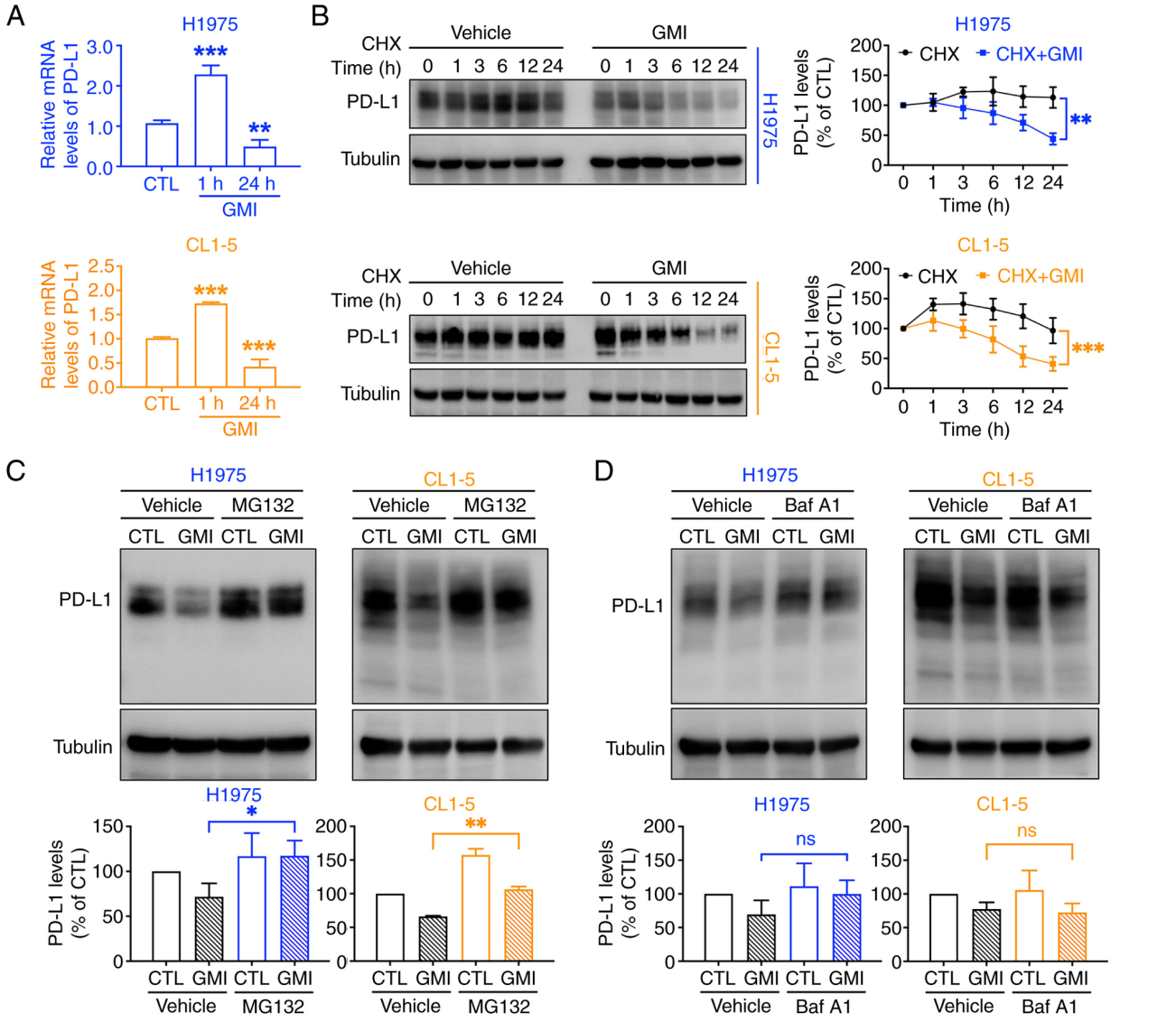

Figure 3. GMI induces proteasome-dependent degradation of PD-L1. (A) Reverse transcription-quantitative PCR analysis of PD-L1 mRNA expression in H1975 and CL1-5 cells following treatment with 0.6 μM GMI for 1 and 24 h. (B) CHX chase assay of H1975 and CL1-5 cells exposed to 200 μg/ml CHX for 30 min, followed by incubation with or without 0.6 μM GMI for the indicated time points to assess PD-L1 protein stability. (C and D) H1975 and CL1-5 cells were pretreated with 10 μM MG132 (C), a proteasome inhibitor, or 5 nM Baf A1 (D), a lysosome inhibitor, and were then exposed to 0.6 μM GMI for 24 h. Data are presented as the mean ± standard deviation from three independent experiments. *P<0.05, **P<0.01 and ***P<0.001. GMI, *Ganoderma microsporum* immunomodulatory protein; PD-L1, programmed death-ligand 1; CHX, cycloheximide; Baf A1, bafilomycin A1; ns, not significant.

utilized, where murine PD-L1 (mPD-L1) was replaced with hPD-L1 (Figs. 5C and S2A). GMI suppressed PD-L1 levels in LLC1-hPD-L1 cells *in vitro* (Fig. S7A) and promoted PD-L1 degradation through the ubiquitin-mediated proteasomal pathway, consistent with observations in H1975 and CL1-5 cells (Fig. S7B and C). LLC1-hPD-L1 cells were subcutaneously inoculated into C57BL/6 mice to evaluate the *in vivo* efficacy of GMI (Fig. 5D). Treatment with GMI significantly inhibited tumor growth and reduced tumor weight without causing body weight loss (Figs. 5E-G and S7D). Tumor tissue analysis confirmed GMI-mediated downregulation of PD-L1 expression (Fig. 5H). These findings indicated that GMI suppresses PD-L1 expression and may enhance antitumor immunity by facilitating PD-L1 degradation in tumor-bearing mice.

T cell suppresses the viability of GMI-pretreated cancer cells. The binding of PD-L1 on cancer cell membranes to PD-1 on T cells suppresses T cell activation, facilitating immune evasion and tumor progression (38). Given the previous finding that GMI promotes PD-L1 degradation on cancer cell surfaces, it was hypothesized that this would enhance secretion of T cell cytokines, such as IL-2 and granzyme B, thereby boosting the cytotoxic response against tumor cells (29). To test this, co-culture experiments were performed using T cells isolated from the spleens of LLC1 tumor-bearing mice (Fig. 6A). Activated spleen-derived T cells significantly suppressed the viability of GMI-treated LLC1 cells compared with untreated controls (Fig. 6B). Next, lung cancer cell lines H1975 and PC9, both harboring *EGFR* mutations and stably expressing GFP, were pre-treated with GMI and co-cultured with CD3/CD28-activated Jurkat T cells (29). This co-culture led to a significant increase in IL-2 and granzyme B secretion compared with co-cultures without GMI pretreatment (Fig. S8A and B). Furthermore, tumor-eliminating activity assessed by

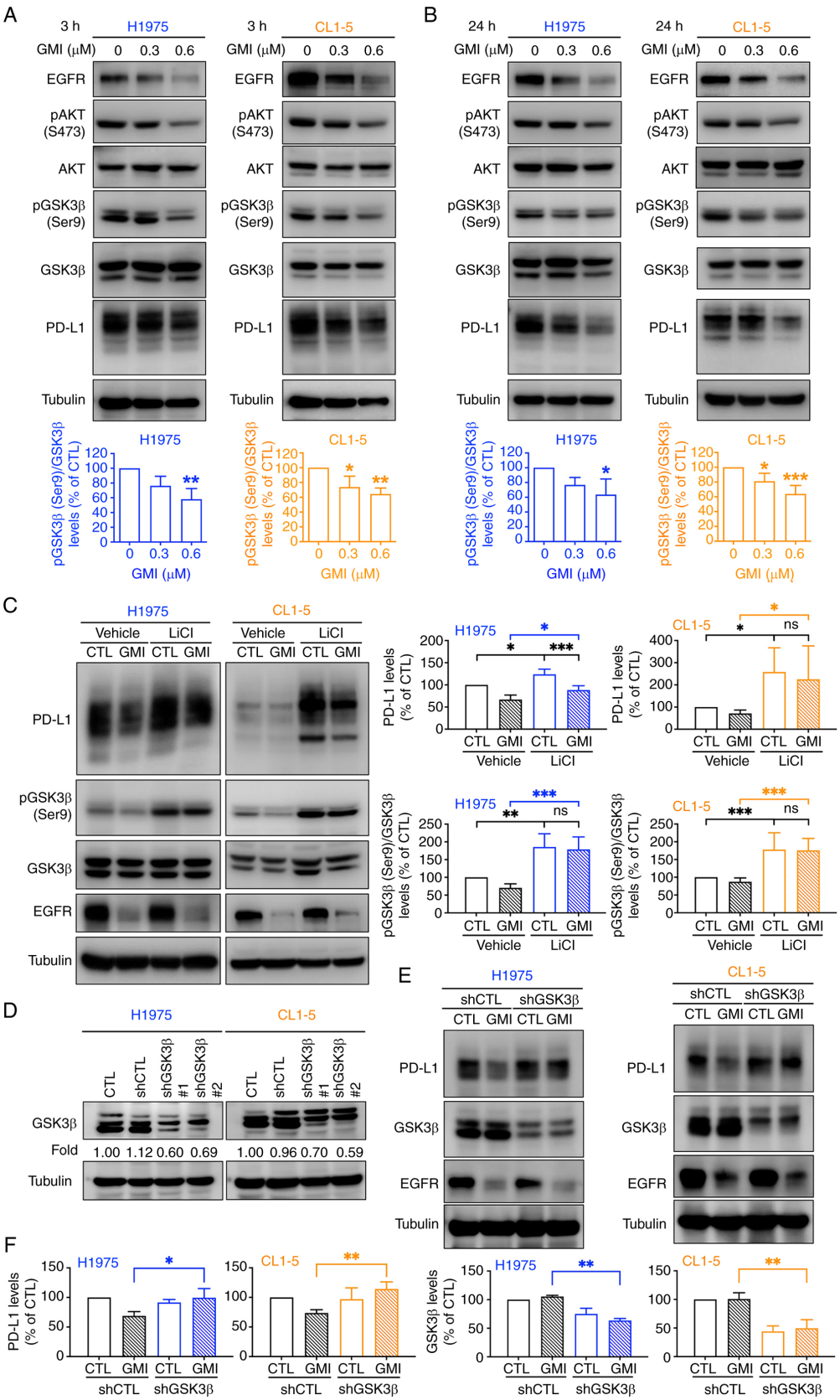

Figure 4. GMI facilitates PD-L1 degradation through activation of GSK3β. (A and B) H1975 and CL1-5 cells were treated with indicated concentrations of GMI for 3 h (A) and 24 h (B). Protein expressions of EGFR, p-AKT (Ser473), p-GSK3β (Ser9) and PD-L1 were analyzed by immunoblotting, with AKT, GSK3β and tubulin as loading controls, and quantification of p-AKT and p-GSK3β was performed relative to their corresponding total proteins (AKT and GSK3β). (C) H1975 and CL1-5 cells were pretreated with 25 mM LiCl, a GSK3β inhibitor, and were exposed to 0.6 μM GMI for 24 h. (D) Immunoblotting of GSK3β in H1975 and CL1-5 cells expressing different GSK3β-targeting shRNAs. (E) Immunoblotting analysis of PD-L1 and GSK3β in cancer cells transduced with either GSK3β shRNA (shGSK3β#1) or control shRNA (shCTL) lentiviruses and treated with or without 0.6 μM GMI for 24 h. (F) Quantification of PD-L1 and GSK3β expression levels shown in (E). Data are presented as the mean ± standard deviation from three independent experiments. *P<0.05, **P<0.01 and ***P<0.001. GMI, *Ganoderma microsporum* immunomodulatory protein; PD-L1, programmed death-ligand 1; p-, phosphorylated; LiCl, lithium chloride; shRNA, short hairpin RNA; p-, phosphorylated; ns, not significant.

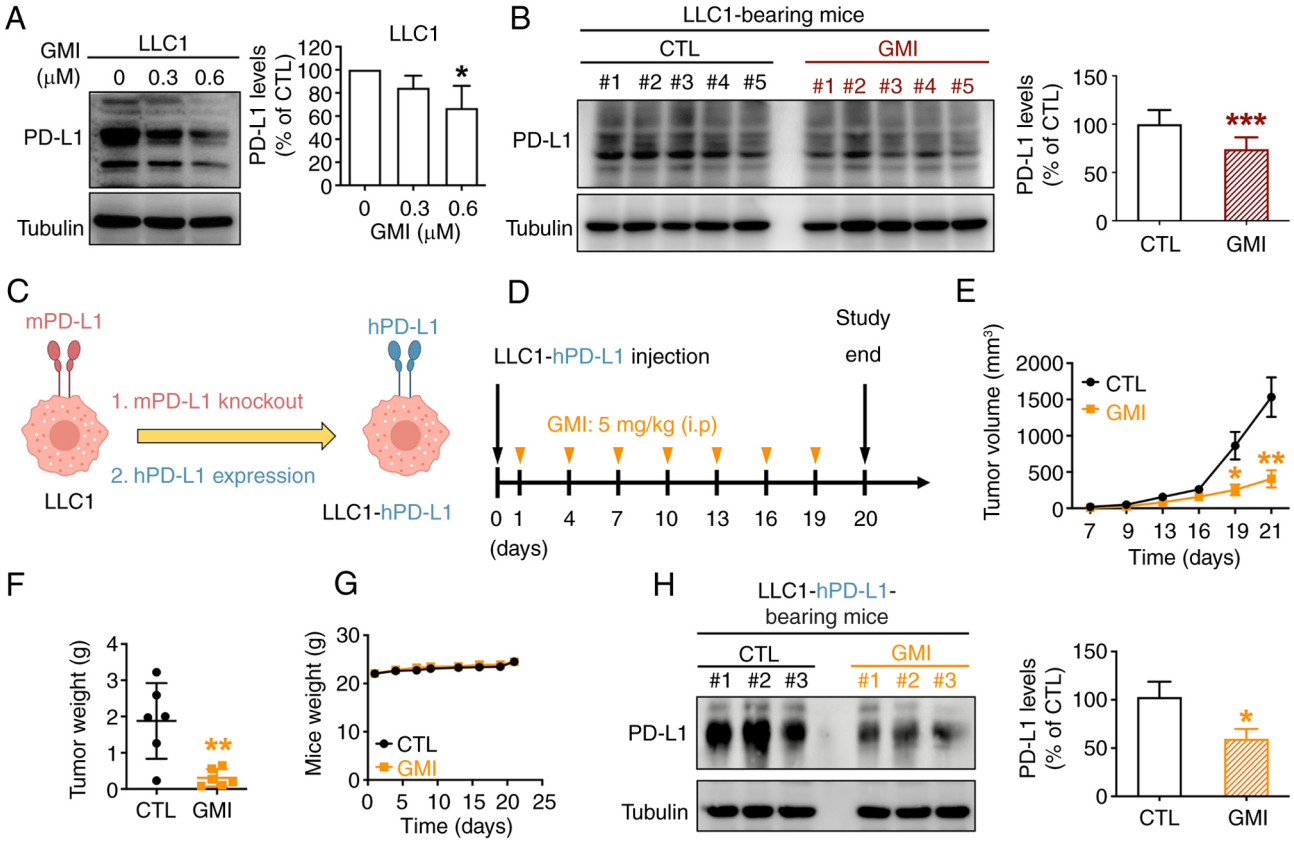

Figure 5. GMI inhibits tumor growth and downregulates PD-L1 in LLC1-hPD-L1 allograft models. (A) LLC1 cells were treated with the indicated concentrations of GMI for 3 h. PD-L1 protein levels were assessed by western blotting, with tubulin as the loading control. Data are presented as the mean ± standard deviation from three independent experiments. (B) Western blot analysis of PD-L1 protein levels in tumor cells harvested from CTL and GMI-treated groups. Quantitative data are shown. (C) Schematic diagram illustrating the knockout of mouse PD-L1 and replacement with human PD-L1 expression. (D) Treatment schedule of LLC1-hPD-L1 syngeneic C57BL/6 mice. Mice were administered intraperitoneal injections of GMI (5.0 mg/kg) every 3 days. (E-G) Tumor volume (E), tumor weight (F) and body weight (G) were measured at the indicated time points. Data are presented as the mean ± SEM (n=6 mice per group). (H) PD-L1 protein levels in excised tumors from CTL and GMI groups were analyzed by western blotting (random samples from 3 mice per group). *P<0.05, **P<0.01 and ***P<0.001. GMI, *Ganoderma microsporum* immunomodulatory protein; PD-L1, programmed death-ligand 1; mPD-L1, mouse PD-L1; hPD-L1, human PD-L1.

relative fluorescence intensity showed a significant decrease in viability of GMI-pretreated lung cancer cells co-cultured with CD3/CD28-stimulated Jurkat T cells (Figs. S8C-E). These results suggested that GMI-mediated reduction of membrane PD-L1 may enhance CD3/CD28-stimulated T cell suppression of cancer cell viability. Interestingly, without tumor cells, GMI elevated CD69 expression and enhanced IL-2 secretion in Jurkat T cells (Fig. S8F and G), indicating a direct stimulatory effect on T cells. In addition, the presence of TILs, including $CD8^+$ and $CD4^+$ T cells, in LLC1 tumor tissues was analyzed (Fig. 5B). Flow cytometry revealed a higher proportion of $CD8^+$ TILs in GMI-treated tumors (Figs. 6C and S9), indicating that GMI may promote the infiltration of activated $CD8^+$ cytotoxic T cells into the TME through PD-L1 degradation. Collectively, the aforementioned findings suggested that GMI-facilitated PD-L1 degradation may promote antitumor immunity.

Finally, analysis on whether combining GMI with PD-1 blockade (Fig. 6D) can further enhance antitumor efficacy revealed that combination treatment (GMI + anti-PD-1 mAb) significantly suppressed tumor growth (Fig. 6E) and reduced tumor weight (Figs. 6F and S10) compared with the control (PBS) group. However, tumor suppression in the combined treatment group was not significantly different from the GMI-only group. Furthermore, in line with our earlier findings from the syngeneic mouse model, body weights remained stable across all groups (Fig. 6G), indicating that GMI is safe for promoting PD-L1 degradation as a therapeutic strategy.

Discussion

PD-L1 on tumor cells interacts with the PD-1 receptor on T lymphocytes, a key mechanism of immune evasion in multiple cancer types. This interaction effectively suppresses the immune system's ability to detect and eliminate malignant cells, contributing to tumor progression. The development and approval of multiple antibodies targeting the PD-1/PD-L1 pathway represent a major advancement in cancer immunotherapy by disrupting this immune checkpoint and restoring immune function in patients (39). Beyond inhibiting the PD-1/PD-L1 interaction between cancer cells and immune T cells, a more direct strategy targeting PD-L degradation has gained attention. By reducing PD-L1 expression on tumor cell surface, this approach may diminish immune evasion and strengthen antitumor immunity, positioning PD-L1 degradation as a promising therapeutic avenue (40). Since EGFR activation stabilizes PD-L1 by inhibiting its degradation, agents targeting

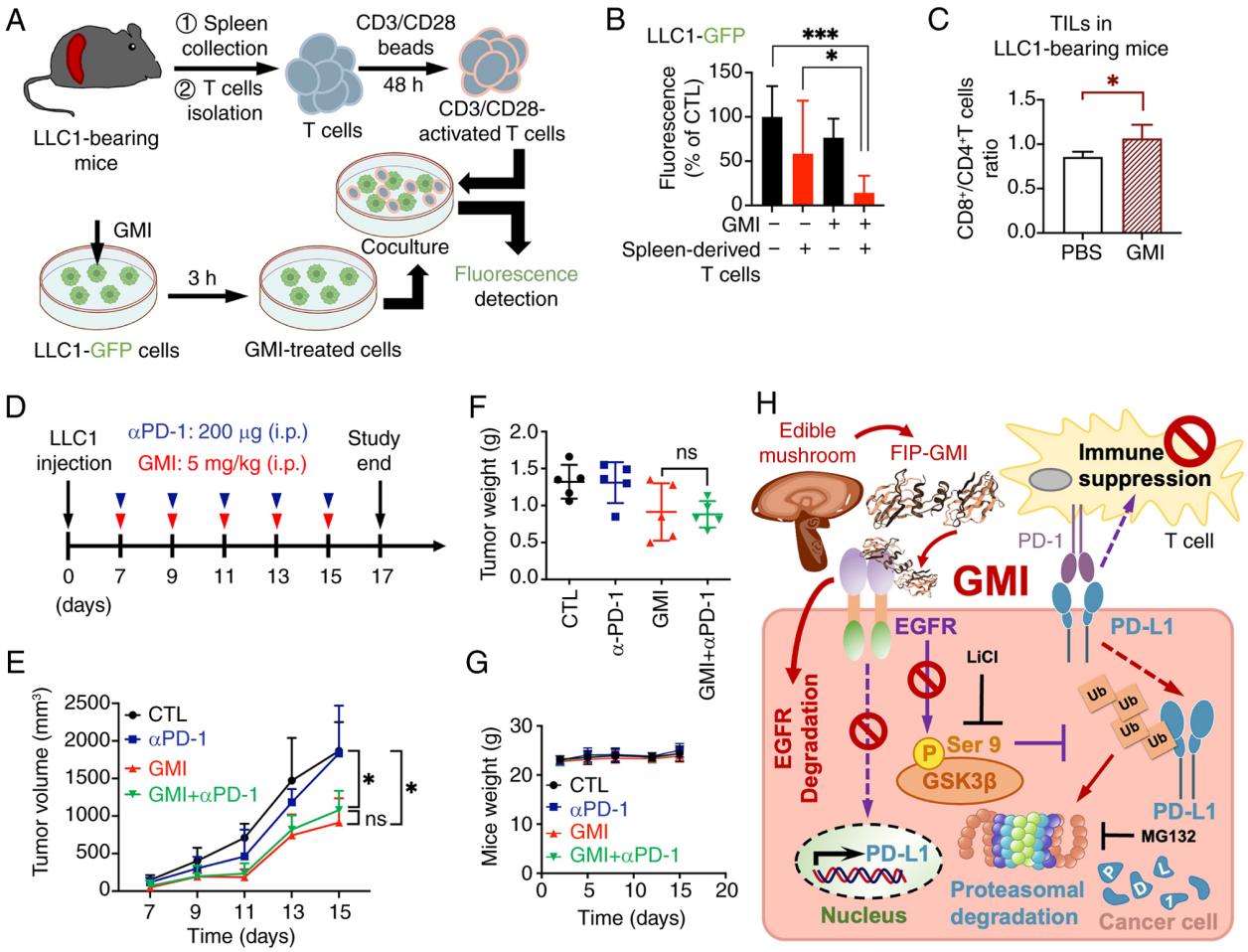

Figure 6. GMI regulates T cell-mediated suppression of tumor cells *ex vivo* and promotes antitumor immunity *in vivo*. (A) Schematic diagram illustrating the co-culture protocol. Activated spleen-derived T cells isolated from LLC1-bearing mice were co-cultured with LLC1-GFP cells pretreated with 0.6 μM GMI for 3 h. After 72 h of co-culture, GFP fluorescence in LLC1-GFP cells was analyzed. (B) Quantification of GFP fluorescence intensity in LLC1-GFP cells following co-culture with activated T cells. (C) Flow cytometric analysis of tumor-infiltrating lymphocytes from LLC1-bearing mice treated with control (PBS) or GMI (Fig. 5B). The ratio of $CD8^+$ to $CD4^+$ T cells is shown. (D) Treatment schedule for LLC1 syngeneic C57BL/6 mice receiving intraperitoneal injections of GMI (5.0 mg/kg), anti-PD-1 antibody (200 μg/mice), or their combination every 2 days. (E-G) Tumor volume (E), tumor weight (F) and body weight (G) were monitored at specified intervals throughout the experiment. Data are presented as the mean ± SEM (n=5 mice per group). (H) Schematic model illustrating how GMI enhances antitumor immunity by driving PD-L1 breakdown. GMI, a FIP derived from an edible mushroom and known as an EGFR degrader, reduces PD-L1 levels by downregulating its mRNA expression and promoting GSK3β-mediated ubiquitination and proteasomal degradation. This process further diminishes T cell immune suppression and enhances antitumor immunity. *P<0.05 and ***P<0.001. *Ganoderma microsporum* immunomodulatory protein; GFP, green fluorescent protein; PD-1, programmed cell death protein-1; FIPs, fungal immunomodulatory proteins; LiCl, lithium chloride; ns, not significant.

the EGFR pathway can modulate PD-L1 levels (12). Bioactive compounds derived from medicinal mushrooms, including FIPs and polysaccharides, have attracted considerable interest for their therapeutic potential, particularly in cancer treatment (41). To the best of our knowledge, the present study is the first to demonstrate that FIP-GMI, an approved dietary ingredient and EGFR degrader, regulates antitumor immunity by promoting PD-L1 degradation (Fig. 6H). Notably, previous studies by the authors revealed that GMI can induce proteasomal degradation of key proteins, including EGFR and Slug in lung and brain cancer cells (18,19), and ACE2 in SARS-CoV-2 infection models (20). In the present study, it was further demonstrated that GMI facilitates GSK3β-mediated proteasomal degradation of PD-L1, suggesting that GMI targets multiple substrates through this pathway across various cell types. Moreover, proteomic analysis revealed that GMI regulates a broad spectrum of membrane proteins (Fig. 1A), though the precise mechanisms remain to be elucidated.

PD-L1 transcription is regulated by various transcription factors. Notably, c-Myc binds directly to the PD-L1 gene promoter, with its inhibition reducing both PD-L1 mRNA and protein levels, thereby boosting antitumor immunity (42). Similarly, Hippo pathway effectors, such as the transcriptional activator yes-associated protein and signal transducer and activator of transcription 3 (STAT3), have been shown to regulate PD-L1 transcription in various cancer types (43,44). EGFR inhibitors significantly suppress PD-L1 mRNA in lung cancer cells with activating mutations (14,45) and block EGF-induced PD-L1 upregulation, indicating that inhibiting EGFR activity regulates PD-L1 mRNA expression. Previous research has shown that GMI reduces STAT3 phosphorylation, hinting at transcriptional regulation of PD-L1 (31). The current findings confirmed that GMI significantly downregulates PD-L1 mRNA expression in lung cancer cells within 24 h, likely by targeting these critical transcriptional regulators. Additional investigations could be carried out to examine how

GMI influences these transcription factors involved in regulating PD-L1 mRNA. Moreover, other signaling pathways, including those involving receptor tyrosine kinases (RTKs) such as anaplastic lymphoma kinase (46) and neurotrophic RTK 1 (47), as well as the PI3K-AKT-mTOR axis (48), also upregulate both PD-L1 mRNA and protein expression.

Beyond transcriptional regulation, GMI promotes PD-L1 degradation via GSK3β activity in lung cancer cells. Future investigations could explore whether GMI exerts effects on broader immune checkpoint regulatory pathways, extending beyond GSK3β, and further evaluate its potential to disrupt both transcriptional and post-translational processes governing PD-L1 expression.

GSK3β facilitates PD-L1 identification by the E3 ubiquitin ligase complex, which encompasses beta-transducing repeat-containing protein (β-TrCP), leading to ubiquitination and proteasomal degradation. By contrast, EGFR activation inhibits GSK3β via AKT-mediated phosphorylation, stabilizing PD-L1 and promoting immune resistance (12). EGFR inhibitors, such as gefitinib and osimertinib, counteract this stabilization effect by blocking EGFR signaling, which can activate GSK3β (45). Consistently, the present study demonstrated that GMI, the EGFR degrader, activates GSK3β, and GSK3β inhibition or knockdown reverses GMI-induced PD-L1 reduction, confirming its crucial role. Of note, short-term EGF exposure partially rescued GMI-induced GSK3β activation (data not shown); however, an EGFR overexpression rescue experiment was not performed, suggesting that other RTKs may also regulate GSK3β activity. Contrary to the previous study (12), the present findings revealed that β-TrCP knockdown did not fully prevent PD-L1 degradation by GMI (data not shown), suggesting involvement of alternative E3 ubiquitin ligases. Candidates include membrane-associated RING-CH 8 (MARCH8) and ariadne-1 homolog (ARIH1), which mediate PD-L1 degradation in EGFR-mutant NSCLC cells exposed to EGFR inhibitors (14,49). Thus, GMI appears to regulate PD-L1 via a β-TrCP-independent yet GSK3β-dependent mechanism, warranting further exploration of novel E3 ubiquitin ligases involved in GMI-mediated PD-L1 degradation.

Numerous PD-L1-targeting strategies, such as proteolysis-targeting chimeras, lysosomal-targeted chimeras and GlueBody chimeras, have shown considerable promise in promoting PD-L1 degradation (50,51). However, these approaches often face limitations associated with suboptimal drug delivery efficiency, large molecular size and restricted tumor tissue penetration (52). By contrast, GMI is a naturally derived FIP with a favorable safety profile (53). The findings of the present study demonstrated that GMI effectively downregulates PD-L1 expression by repressing its transcription and enhancing GSK3β-mediated proteasomal degradation. Unlike synthetic degraders that frequently require intricate molecular design and chemical modification, GMI offers potential advantages in terms of biocompatibility, low toxicity and feasibility as a functional dietary supplement. Overall, these characteristics underscore the therapeutic significance of GMI and support its promise as a novel and practical alternative to existing PD-L1-targeting approaches.

Immune resistance and the immunosuppressive TME remain major challenges in treating solid tumors (54). Elevated PD-L1 correlates with tumor progression, reduced T-cell activity, and the development of immune evasion. A promising therapeutic strategy that disrupts PD-L1/PD-1 binding can re-engage T cell-mediated immunity. Promoting PD-L1 degradation enhances immune responses and T cell function, thereby improving therapeutic outcomes (55). The aqueous extract derived from the medicinal herb *Centipeda minima* alleviates tumor burden in mice harboring NSCLC cells by regulating PD-L1 expression and enhancing $CD8^+$ T cell cytotoxicity (56). Moreover, the natural marine compound benzosceptrin C strongly promotes PD-L1 degradation and exerts immune antitumor effects, effectively inhibiting tumor growth in MC38 tumor-bearing mice (57). Collectively, these studies indicate that using active compounds from natural products or traditional Chinese medicine herbs may offer promising therapeutic strategies for combating tumors and enhancing antitumor immunity. Furthermore, FIPs, including FIP-vvo derived from *Volvariella volvacea*, modulate immune responses and may support health by boosting immune function (58). The present study introduces fungal-derived GMI as a novel PD-L1 degrader. *In vitro* co-cultures showed that GMI effectively reduces PD-L1 in cancer cells, significantly enhancing CD3/CD28-stimulated T cell-mediated suppression of cancer cell viability. Consistently, *in vivo* experiments demonstrated significant tumor growth inhibition accompanied by increased infiltration of $CD8^+$ TILs, supporting enhanced antitumor immunity within the TME. Notably, in the absence of tumor cells, GMI upregulated Jurkat T-cell CD69 expression and increased IL-2 secretion (Fig. S8F and G), indicating that, beyond downregulating PD-L1 on tumor cells, GMI directly stimulates T cells and may thereby potentiate antitumor immune responses. Future studies will further explore the molecular mechanisms underlying this direct activation and its implications for cancer immunotherapy.

No synergistic effect was observed when GMI was administered in combination with anti-PD-1 in LLC1-bearing mice, consistent with LLC tumors being relatively 'cold' and resistant to anti-PD-1/PD-L1 therapy (30). This may explain the limited efficacy of anti-PD-1 antibodies in our *in vivo* model. Prior studies indicate that checkpoint inhibitors beyond PD-1/PD-L1, such as CTLA-4 blockade, which modulates the CTLA-4/CD80 (CD86) axis or TIGIT blockade (targeting the TIGIT/PVR axis), can elicit distinct immune responses that vary with tumor type and microenvironment (59). Although CD80 and CD86 were not detected in our proteomic analysis, PVR, an immune checkpoint ligand involved in immune evasion (60), was unexpectedly identified, suggesting that the TIGIT pathway may warrant further investigation. Accordingly, investigating the combination of GMI with blocking antibodies against other immune checkpoints, such as CTLA-4 or TIGIT, presents an intriguing direction for future research to better elucidate potential synergistic effects. It is essential to highlight that no significant weight loss or visible adverse effects were observed in our tumor-bearing model, indicating that GMI is well-tolerated. In addition, recent research by the authors demonstrated that GMI ameliorates SARS-CoV-2 envelope protein-induced inflammation and exerts anti-inflammatory effects in mouse models of excessive immune activation (61). These results suggested that, beyond its role in PD-L1 regulation, GMI may contribute to immune homeostasis, potentially mitigating the risk of immune-related adverse effects. Furthermore, a

favorable safety profile for GMI has been previously demonstrated, further supporting its potential as a safe option in therapeutic applications (53). Collectively, the aforementioned findings support GMI as a valuable supplement in cancer therapy by targeting both tumor growth and immune evasion.

While PD-L1 has traditionally been studied for its role as an immune checkpoint ligand, evidence highlights its tumor cell-intrinsic functions, which may complicate its use as a biomarker for immunotherapy. These intrinsic roles extend beyond immune evasion and include promoting cancer cell survival, invasion, EMT, stemness, metabolic reprogramming and therapy resistance. Emerging studies have shown that PD-L1 can activate intracellular signaling pathways, such as PI3K/AKT and MAPK, which are crucial for cancer cell proliferation and survival (62,63). Moreover, intrinsic PD-L1 activity in tumor cells drives NSCLC progression by facilitating EMT, and elevated EMT levels in PD-L1-high NSCLC may serve as a predictor of poor outcomes following immune checkpoint inhibitor therapy (64). Additionally, PD-L1 has been implicated in enhancing glycolysis, thereby supporting the metabolic demands of rapidly growing tumors (65). Other intrinsic functions include its involvement in the anti-apoptotic processes and chemotherapy resistance, where PD-L1 helps protect cancer cells from these therapeutic agents (66,67). Importantly, previous studies by the authors showed that GMI suppresses lung and brain cancer cell migration and metastasis by inhibiting Slug, a transcription factor associated with EMT (18,22). This mechanism may intersect with PD-L1's roles in promoting EMT and metastasis, highlighting a potential link between GMI's effects and the intrinsic functions of PD-L1. Future studies could clarify whether GMI's suppression of EMT and metastasis is directly mediated through its impact on PD-L1 signaling pathways. Such investigations could provide deeper insights into the dual role of GMI in targeting both the immune and non-immune functions of PD-L1, further advancing its therapeutic potential.

A previous study (19) by the authors demonstrated that GMI is a novel EGFR degrader capable of disrupting EGFR-driven oncogenic signaling and inhibiting tumor progression in EGFR-positive cancers. In xenograft models, GMI effectively suppresses tumor growth in nude mice harboring tumors with both EGFR wild-type and activating mutations, indicating a direct cytotoxic effect (17,19). Notably, in immune-competent mouse models, GMI inhibits tumor metastasis in a tail-vein injection model and suppresses the growth of subcutaneous LLC1 tumors in C57BL/6 mice (22). These findings indicated that, beyond its direct cytotoxic effects, GMI may also exert antitumor activity by enhancing endogenous immune defense mechanisms. Building on this, the current study further demonstrated that GMI suppresses tumor growth and induces PD-L1 downregulation *in vivo*, suggesting a dual mechanism of action. One potential anticancer mechanism of GMI is its ability to enhance antitumor immunity through PD-L1 degradation, thereby alleviating immune suppression. While PD-L1 reduction contributes to enhanced antitumor immunity, tumor suppression in nude mouse models with defective T cell function suggests an additional direct cytotoxic effect. This is consistent with the mechanisms of other FDA-approved EGFR-tyrosine kinase inhibitors, such as osimertinib and erlotinib, which not only disrupt EGFR signaling and induce tumor cell apoptosis but also regulate immune responses by reducing PD-L1 expression and modulating the TME (12,14). The observed reduction in PD-L1 levels and the concurrent increase in $CD8^+$ T cell infiltration in the TME indicated that GMI may exert its effects by modulating the T cell landscape to combat tumors. This suggests that GMI's effects extend beyond simply eliminating cancer cells, potentially encompassing tumor suppression through PD-L1 downregulation on malignant cells.

The present study has several limitations. Firstly, while the co-culture system employing Jurkat T cells and cancer cells represents a well-established and widely adopted approach for assessing the functional activation of Jurkat T cells (68), it fails to fully replicate antigen-specific T cell-mediated antitumor responses or to provide a reliable evaluation of T cell-mediated tumor cell cytotoxicity. Alternative models, such as the co-culture of human peripheral blood mononuclear cells with GMI-treated human cancer cells or the co-culture of OVA-specific T cells with GMI-treated OVA-expressing cancer cells (56), could better elucidate the mechanisms underlying T cell-mediated antitumor immunity in the context of GMI treatment. Secondly, while GMI enhances antitumor immunity by promoting GSK3β-mediated PD-L1 degradation, without a T cell depletion assay, *in vivo* antitumor effects in immune-competent mice remain unclear. In addition, p-GSK3β (Ser9) was not quantified in the tumor samples; therefore, while *in vitro* data support GSK3β-dependent PD-L1 degradation, GSK3β activation *in vivo* could not be directly confirmed in this cohort. Lastly, proteomic analysis revealed that GMI does not significantly alter surface MHC class I (HLA-A/B/C/E/G/F) expression on several lung cancer cell lines following GMI treatment (data not shown), suggesting no direct effect on antigen presentation pathways. However, broader indirect effects on immune modulation require further investigation.

In conclusion, the present study provides evidence for the first time that the naturally derived FIP GMI, beyond its cytotoxic effects as an EGFR degrader, promotes PD-L1 degradation by decreasing its mRNA expression and inducing GSK3β-mediated proteasomal degradation. This reduction of PD-L1 enhances CD3/CD28-stimulated T cell-mediated suppression of cancer cell viability and inhibits tumor growth with increased $CD8^+$ T cell infiltration *in vivo*. Collectively, these results highlight the promising potential of GMI as a therapeutic agent or functional dietary supplement for cancer immunotherapy.

Acknowledgements

The authors are sincerely grateful to Ms Y-C Chen of National Yang Ming Chiao Tung University for providing technical assistance.

Funding

The present study was supported by grants from the Ministry of Science and Technology of Taiwan (grant no. Young Scholar Fellowship Einstein Program; MOST 111-2636-B-A49-009) and the National Science and Technology Council of Taiwan (grant no. NSTC 112-2320-B-A49-010-MY3, NSTC 113-2320-B-A49-028-MY3, NSTC 113-2811-B-A49A-038 and NSTC 114-2811-B-A49A-015).

Availability of data and materials

The data generated in the present study may be requested from the corresponding author. The data generated in the present study may be found in the NYCU Dataverse under accession number 10.57770/QNCRKI or at the following URL: https://doi.org/10.57770/QNCRKI.

Authors' contributions

LLL, WHH and TYL conceptualized the study. WJH performed experiments, collected and analyzed data, interpreted the results, and wrote the manuscript. WJH and LCH performed bioinformatic analysis. LCH, ZHL, YRC and KFL performed *in vitro* and *in vivo* experiments. TYL reviewed and edited the manuscript. WJH and TYL confirm the authenticity of all the raw data. All authors read and approved the final version of the manuscript.

Ethics approval and consent to participate

All procedures involving animals were conducted in accordance with the guidelines established by the Institutional Animal Care and Use Committee (IACUC; approval no. 1070805) at National Yang Ming Chiao Tung University (Taipei, Taiwan).

Patient consent for publication

Not applicable.

Competing interests

The authors declare that they have no competing interests.

References

1. Zou W: Immunosuppressive networks in the tumour environment and their therapeutic relevance. Nat Rev Cancer 5: 263-274, 2005.
2. Han Y, Liu D and Li L: PD-1/PD-L1 pathway: Current researches in cancer. Am J Cancer Res 10: 727-742, 2020.
3. Sun C, Mezzadra R and Schumacher TN: Regulation and function of the PD-L1 checkpoint. Immunity 48: 434-452, 2018.
4. Iwai Y, Hamanishi J, Chamoto K and Honjo T: Cancer immunotherapies targeting the PD-1 signaling pathway. J Biomed Sci 24: 26, 2017.
5. Brahmer JR, Tykodi SS, Chow LQ, Hwu WJ, Topalian SL, Hwu P, Drake CG, Camacho LH, Kauh J, Odunsi K, *et al*: Safety and activity of anti-PD-L1 antibody in patients with advanced cancer. N Engl J Med 366: 2455-2465, 2012.
6. Sharma P and Allison JP: Immune checkpoint targeting in cancer therapy: Toward combination strategies with curative potential. Cell 161: 205-214, 2015.
7. Naidoo J, Page DB, Li BT, Connell LC, Schindler K, Lacouture ME, Postow MA and Wolchok JD: Toxicities of the anti-PD-1 and anti-PD-L1 immune checkpoint antibodies. Ann Oncol 26: 2375-2391, 2015.
8. Zhang N, Dou Y, Liu L, Zhang X, Liu X, Zeng Q, Liu Y, Yin M, Liu X, Deng H and Song D: SA-49, a novel aloperine derivative, induces MITF-dependent lysosomal degradation of PD-L1. EBioMedicine 40: 151-162, 2019.
9. Wang T, Cai S, Cheng Y, Zhang W, Wang M, Sun H, Guo B, Li Z, Xiao Y and Jiang S: Discovery of small-molecule inhibitors of the PD-1/PD-L1 axis that promote PD-L1 internalization and degradation. J Med Chem 65: 3879-3893, 2022.
10. Cha JH, Chan LC, Li CW, Hsu JL and Hung MC: Mechanisms controlling PD-L1 expression in cancer. Mol Cell 76: 359-370, 2019.
11. Hsu JM, Xia W, Hsu YH, Chan LC, Yu WH, Cha JH, Chen CT, Liao HW, Kuo CW, Khoo KH, *et al*: STT3-dependent PD-L1 accumulation on cancer stem cells promotes immune evasion. Nat Commun 9: 1908, 2018.
12. Li CW, Lim SO, Xia W, Lee HH, Chan LC, Kuo CW, Khoo KH, Chang SS, Cha JH, Kim T, *et al*: Glycosylation and stabilization of programmed death ligand-1 suppresses T-cell activity. Nat Commun 7: 12632, 2016.
13. Zhang J, Bu X, Wang H, Zhu Y, Geng Y, Nihira NT, Tan Y, Ci Y, Wu F, Dai X, *et al*: Cyclin D-CDK4 kinase destabilizes PD-L1 via cullin 3-SPOP to control cancer immune surveillance. Nature 553: 91-95, 2018.
14. Qian G, Guo J, Vallega KA, Hu C, Chen Z, Deng Y, Wang Q, Fan S, Ramalingam SS, Owonikoko TK, *et al*: Membrane-associated RING-CH 8 functions as a novel PD-L1 E3 ligase to mediate PD-L1 degradation induced by EGFR inhibitors. Mol Cancer Res 19: 1622-1634, 2021.
15. Su YW, Huang WY, Lin SH and Yang PS: Effects of reishimmune-S, a fungal immunomodulatory peptide supplement, on the quality of life and circulating natural killer cell profiles of patients with early breast cancer receiving adjuvant endocrine therapy. Integr Cancer Ther 23: 15347354241242120, 2024.
16. Lin TY, Hua WJ, Yeh H and Tseng AJ: Functional proteomic analysis reveals that fungal immunomodulatory protein reduced expressions of heat shock proteins correlates to apoptosis in lung cancer cells. Phytomedicine 80: 153384, 2021.
17. Hua WJ, Hwang WL, Yeh H, Lin ZH, Hsu WH and Lin TY: Ganoderma microsporum immunomodulatory protein combined with KRAS(G12C) inhibitor impedes intracellular AKT/ERK network to suppress lung cancer cells with KRAS mutation. Int J Biol Macromol 259: 129291, 2024.
18. Tseng AJ, Tu TH, Hua WJ, Yeh H, Chen CJ, Lin ZH, Hsu WH, Chen YL, Hsu CC and Lin TY: GMI, Ganoderma microsporum protein, suppresses cell mobility and increases temozolomide sensitivity through induction of Slug degradation in glioblastoma multiforme cells. Int J Biol Macromol 219: 940-948, 2022.
19. Hua WJ, Yeh H, Lin ZH, Tseng AJ, Huang LC, Qiu WL, Tu TH, Wang DH, Hsu WH, Hwang WL and Lin TY: Ganoderma microsporum immunomodulatory protein as an extracellular epidermal growth factor receptor (EGFR) degrader for suppressing EGFR-positive lung cancer cells. Cancer Lett 578: 216458, 2023.
20. Yeh H, Vo DNK, Lin ZH, Ho HPT, Hua WJ, Qiu WL, Tsai MH and Lin TY: GMI, a protein from Ganoderma microsporum, induces ACE2 degradation to alleviate infection of SARS-CoV-2 Spike-pseudotyped virus. Phytomedicine 103: 154215, 2022.
21. Allen M, Bjerke M, Edlund H, Nelander S and Westermark B: Origin of the U87MG glioma cell line: Good news and bad news. Sci Transl Med 8: 354re353, 2016.
22. Lo HC, Hua WJ, Yeh H, Lin ZH, Huang LC, Ciou YR, Ruan R, Lin KF, Tseng AJ, Wu ATH, *et al*: GMI, a Ganoderma microsporum protein, abolishes focal adhesion network to reduce cell migration and metastasis of lung cancer. Life Sci 335: 122255, 2023.
23. Ge SX, Jung D and Yao R: ShinyGO: A graphical gene-set enrichment tool for animals and plants. Bioinformatics 36: 2628-2629, 2020.
24. Luo W and Brouwer C: Pathview: An R/Bioconductor package for pathway-based data integration and visualization. Bioinformatics 29: 1830-1831, 2013.
25. Kanehisa M, Furumichi M, Sato Y, Ishiguro-Watanabe M and Tanabe M: KEGG: Integrating viruses and cellular organisms. Nucleic Acids Res 49: D545-D551, 2021.
26. Hsu WH, Hua WJ, Qiu WL, Tseng AJ, Cheng HC and Lin TY: WSG, a glucose-enriched polysaccharide from Ganoderma lucidum, suppresses tongue cancer cells via inhibition of EGFR-mediated signaling and potentiates cisplatin-induced apoptosis. Int J Biol Macromol 193: 1201-1208, 2021.
27. Livak KJ and Schmittgen TD: Analysis of relative gene expression data using real-time quantitative PCR and the 2(-Delta Delta C(T)) method. Methods 25: 402-408, 2001.
28. Zhang Y, Huang Y, Yu D, Xu M, Hu H, Zhang Q, Cai M, Geng X, Zhang H, Xia J, *et al*: Demethylzeylasteral induces PD-L1 ubiquitin-proteasome degradation and promotes antitumor immunity via targeting USP22. Acta Pharm Sin B 14: 4312-4328, 2024.
29. Lu CS, Lin CW, Chang YH, Chen HY, Chung WC, Lai WY, Ho CC, Wang TH, Chen CY, Yeh CL, *et al*: Antimetabolite pemetrexed primes a favorable tumor microenvironment for immune checkpoint blockade therapy. J Immunother Cancer 8: e001392, 2020.

30. He K, Barsoumian HB, Puebla-Osorio N, Hu Y, Sezen D, Wasley MD, Bertolet G, Zhang J, Leuschner C, Yang L, *et al*: Inhibition of STAT6 with antisense oligonucleotides enhances the systemic antitumor effects of radiotherapy and Anti-PD-1 in metastatic non-small cell lung cancer. Cancer Immunol Res 11: 486-500, 2023.
31. Wang TY, Yu CC, Hsieh PL, Liao YW, Yu CH and Chou MY: GMI ablates cancer stemness and cisplatin resistance in oral carcinomas stem cells through IL-6/Stat3 signaling inhibition. Oncotarget 8: 70422-70430, 2017.
32. Lin TY, Hsu HY, Sun WH, Wu TH and Tsao SM: Induction of Cbl-dependent epidermal growth factor receptor degradation in Ling Zhi-8 suppressed lung cancer. Int J Cancer 140: 2596-2607, 2017.
33. Hsin IL, Chiu LY, Ou CC, Wu WJ, Sheu GT and Ko JL: CD133 inhibition via autophagic degradation in pemetrexed-resistant lung cancer cells by GMI, a fungal immunomodulatory protein from Ganoderma microsporum. Br J Cancer 123: 449-458, 2020.
34. Lin PL, Wu TC, Wu DW, Wang L, Chen CY and Lee H: An increase in BAG-1 by PD-L1 confers resistance to tyrosine kinase inhibitor in non-small cell lung cancer via persistent activation of ERK signalling. Eur J Cancer 85: 95-105, 2017.
35. Liu M, Wang X, Li W, Yu X, Flores-Villanueva P, Xu-Monette ZY, Li L, Zhang M, Young KH, Ma X and Li Y: Targeting PD-L1 in non-small cell lung cancer using CAR T cells. Oncogenesis 9: 72, 2020.
36. Lemma EY, Letian A, Altorki NK and McGraw TE: Regulation of PD-L1 trafficking from synthesis to degradation. Cancer Immunol Res 11: 866-874, 2023.
37. Feng C, Zhang L, Chang X, Qin D and Zhang T: Regulation of post-translational modification of PD-L1 and advances in tumor immunotherapy. Front Immunol 14: 1230135, 2023.
38. Zuazo M, Gato-Cañas M, Llorente N, Ibañez-Vea M, Arasanz H, Kochan G and Escors D: Molecular mechanisms of programmed cell death-1 dependent T cell suppression: Relevance for immunotherapy. Ann Transl Med 5: 385, 2017.
39. Ghosh C, Luong G and Sun Y: A snapshot of the PD-1/PD-L1 pathway. J Cancer 12: 2735-2746, 2021.
40. Gou Q, Dong C, Xu H, Khan B, Jin J, Liu Q, Shi J and Hou Y: PD-L1 degradation pathway and immunotherapy for cancer. Cell Death Dis 11: 955, 2020.
41. Venturella G, Ferraro V, Cirlincione F and Gargano ML: Medicinal Mushrooms: Bioactive Compounds, Use, and Clinical Trials. Int J Mol Sci 22, 2021.
42. Casey SC, Tong L, Li Y, Do R, Walz S, Fitzgerald KN, Gouw AM, Baylot V, Gütgemann I, Eilers M and Felsher DW: MYC regulates the antitumor immune response through CD47 and PD-L1. Science 352: 227-231, 2016.
43. Miao J, Hsu PC, Yang YL, Xu Z, Dai Y, Wang Y, Chan G, Huang Z, Hu B, Li H, *et al*: YAP regulates PD-L1 expression in human NSCLC cells. Oncotarget 8: 114576-114587, 2017.
44. Zhang N, Zeng Y, Du W, Zhu J, Shen D, Liu Z and Huang JA: The EGFR pathway is involved in the regulation of PD-L1 expression via the IL-6/JAK/STAT3 signaling pathway in EGFR-mutated non-small cell lung cancer. Int J Oncol 49: 1360-1368, 2016.
45. Jiang XM, Xu YL, Huang MY, Zhang LL, Su MX, Chen X and Lu JJ: Osimertinib (AZD9291) decreases programmed death ligand-1 in EGFR-mutated non-small cell lung cancer cells. Acta Pharmacol Sin 38: 1512-1520, 2017.
46. Ota K, Azuma K, Kawahara A, Hattori S, Iwama E, Tanizaki J, Harada T, Matsumoto K, Takayama K, Takamori S, *et al*: Induction of PD-L1 expression by the EML4-ALK oncoprotein and downstream signaling pathways in non-small cell lung cancer. Clin Cancer Res 21: 4014-4021, 2015.
47. Konen JM, Rodriguez BL, Fradette JJ, Gibson L, Davis D, Minelli R, Peoples MD, Kovacs J, Carugo A, Bristow C, *et al*: Ntrk1 promotes resistance to PD-1 checkpoint blockade in mesenchymal Kras/p53 mutant lung cancer. Cancers (Basel) 11: 462, 2019.
48. Lastwika KJ, Wilson W III, Li QK, Norris J, Xu H, Ghazarian SR, Kitagawa H, Kawabata S, Taube JM, Yao S, *et al*: Control of PD-L1 expression by oncogenic activation of the AKT-mTOR pathway in non-small cell lung cancer. Cancer Res 76: 227-238, 2016.
49. Wu Y, Zhang C, Liu X, He Z, Shan B, Zeng Q, Zhao Q, Zhu H, Liao H, Cen X, *et al*: ARIH1 signaling promotes antitumor immunity by targeting PD-L1 for proteasomal degradation. Nat Commun 12: 2346, 2021.
50. Ren X, Wang L, Liu L and Liu J: PTMs of PD-1/PD-L1 and PROTACs application for improving cancer immunotherapy. Front Immunol 15: 1392546, 2024.
51. Zhang F, Jiang R, Sun S, Wu C, Yu Q, Awadasseid A, Wang J and Zhang W: Recent advances and mechanisms of action of PD-L1 degraders as potential therapeutic agents. Eur J Med Chem 268: 116267, 2024.
52. Gao H, Sun X and Rao Y: PROTAC technology: Opportunities and challenges. ACS Med Chem Lett 11: 237-240, 2020.
53. Fu HY and Hseu RS: Safety assessment of the fungal immunomodulatory protein from Ganoderma microsporum (GMI) derived from engineered Pichia pastoris: Genetic toxicology, a 13-week oral gavage toxicity study, and an embryo-fetal developmental toxicity study in Sprague-Dawley rats. Toxicol Rep 9: 1240-1254, 2022.
54. Spitzer MH, Carmi Y, Reticker-Flynn NE, Kwek SS, Madhireddy D, Martins MM, Gherardini PF, Prestwood TR, Chabon J, Bendall SC, *et al*: systemic immunity is required for effective cancer immunotherapy. Cell 168: 487-502, 2017.
55. Yi M, Niu M, Xu L, Luo S and Wu K: Regulation of PD-L1 expression in the tumor microenvironment. J Hematol Oncol 14: 10, 2021.
56. Wang M, Guo H, Sun BB, Jie XL, Shi XY, Liu YQ, Shi XL, Ding LQ, Xue PH, Qiu F, *et al*: Centipeda minima and 6-O-angeloylplenolin enhance the efficacy of immune checkpoint inhibitors in non-small cell lung cancer. Phytomedicine 132: 155825, 2024.
57. Wang Q, Wang J, Yu D, Zhang Q, Hu H, Xu M, Zhang H, Tian S, Zheng G, Lu D, *et al*: Benzosceptrin C induces lysosomal degradation of PD-L1 and promotes antitumor immunity by targeting DHHC3. Cell Rep Med 5: 101357, 2024.
58. Li JP, Lee YP, Ma JC, Liu BR, Hsieh NT, Chen DC, Chu CL and You RI: The enhancing effect of fungal immunomodulatory protein-volvariella volvacea (FIP-vvo) on maturation and function of mouse dendritic cells. Life (Basel) 11: 471, 2021.
59. Sharma P, Goswami S, Raychaudhuri D, Siddiqui BA, Singh P, Nagarajan A, Liu J, Subudhi SK, Poon C, Gant KL, *et al*: Immune checkpoint therapy-current perspectives and future directions. Cell 186: 1652-1669, 2023.
60. Freed-Pastor WA, Lambert LJ, Ely ZA, Pattada NB, Bhutkar A, Eng G, Mercer KL, Garcia AP, Lin L, Rideout WM III, *et al*: The CD155/TIGIT axis promotes and maintains immune evasion in neoantigen-expressing pancreatic cancer. Cancer Cell 39: 1342-1360, 2021.
61. Lin ZH, Yeh H, Lo HC, Hua WJ, Ni MY, Wang LK, Chang TT, Yang MH and Lin TY: GMI, a fungal immunomodulatory protein, ameliorates SARS-CoV-2 envelope protein-induced inflammation in macrophages via inhibition of MAPK pathway. Int J Biol Macromol 241: 124648, 2023.
62. Almozyan S, Colak D, Mansour F, Alaiya A, Al-Harazi O, Qattan A, Al-Mohanna F, Al-Alwan M and Ghebeh H: PD-L1 promotes OCT4 and Nanog expression in breast cancer stem cells by sustaining PI3K/AKT pathway activation. Int J Cancer 141: 1402-1412, 2017.
63. Gao L, Guo Q, Li X, Yang X, Ni H, Wang T, Zhao Q, Liu H, Xing Y, Xi T and Zheng L: MiR-873/PD-L1 axis regulates the stemness of breast cancer cells. EBioMedicine 41: 395-407, 2019.
64. Jeong H, Koh J, Kim S, Song SG, Lee SH, Jeon Y, Lee CH, Keam B, Lee SH, Chung DH and Jeon YK: Epithelial-mesenchymal transition induced by tumor cell-intrinsic PD-L1 signaling predicts a poor response to immune checkpoint inhibitors in PD-L1-high lung cancer. Br J Cancer 131: 23-36, 2024.
65. Chang CH, Qiu J, O'Sullivan D, Buck MD, Noguchi T, Curtis JD, Chen Q, Gindin M, Gubin MM, van der Windt GJ, *et al*: Metabolic competition in the tumor microenvironment is a driver of cancer progression. Cell 162: 1229-1241, 2015.
66. Ghebeh H, Lehe C, Barhoush E, Al-Romaih K, Tulbah A, Al-Alwan M, Hendrayani SF, Manogaran P, Alaiya A, Al-Tweigeri T, *et al*: Doxorubicin downregulates cell surface B7-H1 expression and upregulates its nuclear expression in breast cancer cells: Role of B7-H1 as an anti-apoptotic molecule. Breast Cancer Res 12: R48, 2010.
67. Liu S, Chen S, Yuan W, Wang H, Chen K, Li D and Li D: PD-1/PD-L1 interaction up-regulates MDR1/P-gp expression in breast cancer cells via PI3K/AKT and MAPK/ERK pathways. Oncotarget 8: 99901-99912, 2017.
68. Zheng Y, Fang YC and Li J: PD-L1 expression levels on tumor cells affect their immunosuppressive activity. Oncol Lett 18: 5399-5407, 2019.